Q-switching and mode-locking pulse generation with graphene oxide paper-based saturable absorber

Sulaiman Wadi Harun[1,2], Muhamad Burhan Shah Sabran[1], Salam Mahdi Azooz[2], Ahmad Zarif Zulkifli[2], Mohd Afiq Ismail[2], Harith Ahmad[1]

[1]*Photonics Research Centre, University of Malaya, 50603 Kuala Lumpur, Malaysia*
[2]*Department of Electrical Engineering, Faculty of Engineering, University of Malaya, 50603 Kuala Lumpur, Malaysia*
E-mail: swharun@um.edu.my

Published in *The Journal of Engineering*; Received on 28th November 2014; Accepted on 17th February 2015

Abstract: Q-switched and mode-locked erbium-doped fibre lasers (EDFLs) are demonstrated by using non-conductive graphene oxide (GO) paper as a saturable absorber (SA). A stable and self-starting Q-switched operation was achieved at 1534.4 nm by using a 0.8 m long erbium-doped fibre (EDF) as a gain medium. The pulse repetition rate changed from 14.3 to 31.5 kHz, whereas the corresponding pulse width decreased from 32.8 to 13.8 μs as the pump power increased from 22 to 50.5 mW. A narrow spacing dual-wavelength Q-switched EDFL could also be realised by including a photonics crystal fibre and a tunable Bragg filter in the setup. It can operate at a maximum repetition rate of 31 kHz, with a pulse duration of 7.04 μs and pulse energy of 2.8 nJ. Another GOSA was used to realise mode-locked EDFL in a different cavity consisting of a 1.6 m long EDF in conjunction with 1480 nm pumping. The laser generated a soliton pulse train with a repetition rate of 15.62 MHz and pulse width of 870 fs. It is observed that the proposed fibre lasers have a low pulsing threshold pump power as well as a low damage threshold.

1 Introduction

Pulse fibre lasers have great potential applications in many fields including spectroscopy, biomedical diagnoses, fibre communication and others [1, 2]. Up-to-date, most of the pulse fibre lasers have been realised using passive techniques, where saturable absorbers (SAs) are a key component. Several types of materials and construction techniques have been proposed to develop SAs for lasers. Semiconductor SA mirrors (SESAMs) are the type that are widely used for generating passive Q-switching and mode-locking lasers [3–5]. However, there are still some disadvantages associated with SESAMs, such as limited operation bandwidth and complex fabrication/packaging. As a promising SAs candidate, single walled carbon nanotubes (SWCNTs) have advantages both in recovery time and saturable absorption [6, 7]. To achieve waveband tuning, SWCNTs with different diameters have to be mixed, resulting in extra linear losses, consequently increasing the difficulty of mode locking. As an up and coming material in recent years, graphene possesses favourable characteristics for SAs, similar to SWCNTs. As a result of gapless linear dispersion of Dirac electrons, graphene SAs would achieve wideband, tunable operation without the need of bandgap engineering or chirality/diameter control [8–10]. However, processability is the main issue for graphene-based materials.

Graphene oxide (GO), an example of chemically treated graphene, has attracted much attention recently as a potential alternative to graphene [11]. The structure of GO is composed of sp^2-bonded areas with variable sizes, which are divided by surface oxidation in the form of carboxyl, hydroxyl or epoxy groups. The synthesis of GO is relatively easier than that of graphene, and more importantly, can be prepared in large quantities in both water and organic solvents [11, 12]. Although its electric conductivity is highly influenced by the content of defect clusters, GO has good optical properties. Further investigation shows GO has ultrafast recovery time and strong saturable absorption, which is comparable with that of graphene [13, 14]. Many research works on pulse fibre lasers have also been demonstrated using GO as a SA. GO-based SAs are realised by many techniques such as mirror [15, 16], photonic crystal fibre filled with few-layered GO solution [17], fused silica windows with GO and reduced GO (rGO) layers [18], GO aqueous dispersion [19], reflective GO absorber with glass and copper [20], sandwich structured GO/polyvinyl alcohol (PVA) absorber [21] and GO membrane on microfibre [22].

Recently, a GO paper has been introduced and made available for various applications. It can be prepared by mixing graphite oxide in water. The oxygen atoms of graphite oxide repel water molecules, thus, undergoing complete exfoliation in water, producing colloidal suspensions of almost entirely individual GO sheets. After filtering the exfoliated mixture through a membrane, these GO sheets could be made into paper-like material under a directional flow. A free-standing GO paper is obtained after drying. By changing the oxygen amount on the layers, the material can be an electrical insulator, semiconductor or conductor. This material is uniform and dark brown in colour [11]. In this paper, various pulse fibre lasers are demonstrated using a commercially available non-conductive GO paper as an SA. The easy fabrication of GO paper will promote its potential in Q-switching and mode-locking applications.

2 Preparation of GOSA

GOSA used in this experiment is based on GO paper purchased from Graphene Supermarket at a comparable low price because of its simpler manufacturing process with mass production and has an advantage in terms of mechanical properties [11, 12]. Similar to graphene SA, the implementations of GOSA is performed by depositing or attaching the GO paper into the laser path at one end of the fibre ferrule surface. A common method used to deposit graphene on the fibre ferrule surface is by using optical radiation attraction method [23]. This method is chosen because of the sheet size of the graphene which is too small (typically lateral dimension of 100 nm to few microns in length [24]) to hold and attach to the fibre end surface. GO is however different, the sheet size of the GO is comparably larger (typically lateral dimension of few tens of microns up to few hundreds of microns [25]) making it much easier to handle. A lateral sheet size GO is used to assemble the GOSA in this experiment using laboratory tweezers and placed on the fibre ferrule surface directly. To ensure that the

doi: 10.1049/joe.2014.0321

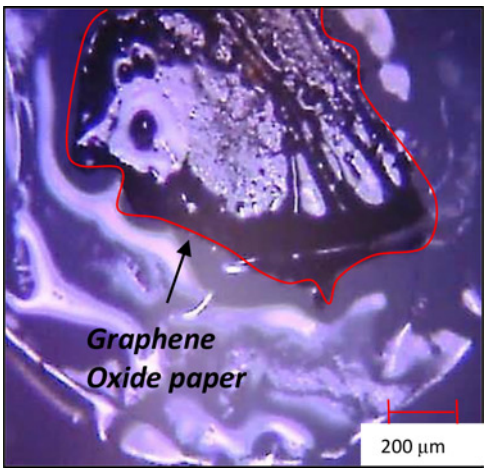

Fig. 1 *Microscopic image of GO paper surrounded by index matching gel*
GO paper sits at the centre of the inner section covering the fibre core

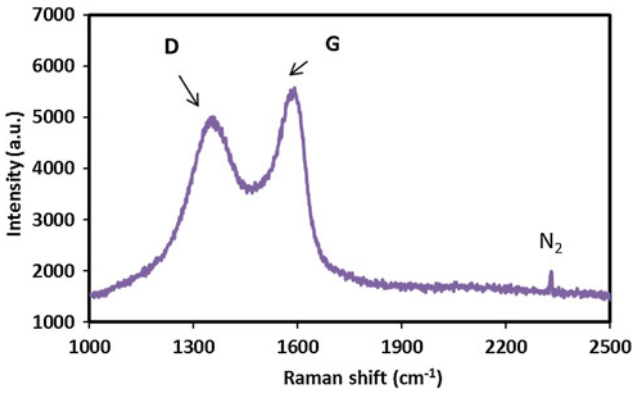

Fig. 2 *Raman spectrum of GO paper measured using Renishaw Raman spectroscopy*

GO paper stick at the centre of the fibre ferrule, a small amount of index matching gel is applied before attaching it. The attached GO paper will cover the fibre end surface. Fig. 1 shows the microscopic image of the GO paper attached to the centre of fibre ferrule covering the laser path with index matching gel surrounding it. The connector will later connect with another connector via ferrule connector/physical contact adapter to sandwich the GO paper to avoid major displacement and form the required SA.

A 50 mW laser at wavelength 532 nm was radiated on the GO paper for a duration of 10 s to generate Raman emission from the GO paper. The Raman spectrum obtained from the Raman spectroscopy scanning is shown in Fig. 2. For rGO and GO, two important bands which are called D (for defect) and G (for graphite) bands should be present. The D-band represents the disorder breaks of the crystal symmetry of carbon sp^2 rings which leads to certain vibrational modes [26]. It is common to all sp^2 carbon lattice and arises from the stretching of C–C bond caused by the incorporation of oxygen O [18]. Meanwhile the G band represents the first-order scattering of the E_{2g} phonon of sp^2 C atoms [27]. The peaks of D and G bands of GO are normally located about 1352 and 1585 cm^{-1}, but in our experiment they were found at ~1353 and 1585.35 cm^{-1}, respectively, in Fig. 2.

As the D-band represents the disorder breaks of the crystal symmetry of carbon sp^2 rings, the graphitic edge related to the GO size will also contribute to the intensity of D-band. The smaller the size of the GO sheets, the higher the peak of the D-band. The relative intensity ratios of both D and G peaks (I_D/I_G) is a measure of disorder degree and is inversely proportional to the average size of the sp^2 clusters which is 0.8971. Although there are disorders caused by the O-incorporation that raise the D peak, it is still relatively low because of the large GO sheet as shown in Fig. 1. The small peak at 2329 cm^{-1} is the N_2 peak which indicates the presence of ambient nitrogen gas. In Fig. 2, the two-dimensional band which is normally used to distinguish the thickness and doping level of the graphene sheets is not observed. This is most probably because of the laser power, which is low as well as the contribution of unintentional doping including O_2 [28].

3 Q-switched erbium-doped fibre laser (EDFL) with GO paper as SA

Fig. 3 shows the experimental setup of the proposed Q-switched EDFL using a ring configuration with a GOSA. A 0.8 m long erbium-doped fibre (EDF) is used as gain medium to provide an amplified spontaneous emission (ASE) at C-band by pumping it with a 980 nm laser diode through a wavelength division multiplexer (WDM). An isolator is used to ensure unidirectional light propagation and the stability of the generated laser. To generate Q-switching pulse train, a GOSA assembly is placed inside the laser cavity as a Q-switcher. A 10 dB coupler is used to tap out 10% of the laser light from the ring cavity. To make accurate measurements, a 3 dB coupler is used to split the laser power into two, where one channel is fixed to a high-resolution optical spectrum analyser (OSA) to monitor the laser output spectrum, whereas the other channel to measure either average output power, time domain and radio-frequency (RF) spectrum.

Initially, the continuous wave (CW) EDFL was investigated without the GOSA and the laser threshold was found to be at the pump power of 18 mW. It should be noted that no Q-switched operation occurs without the GOSA connected in the laser cavity. It is clear that the Q-switched operation is mainly induced by the SA. However, with the GOSA a stable and self-starting Q-switched operation was only observed at the pump power of 22 mW. Fig. 4 shows the optical spectrum of the Q-switched laser at 980 nm pump power of 22 mW. It operates at 1534.4 nm with a signal-to-noise ratio (SNR) of more than 25 dB. For the purpose of comparison, we have also shown the CW lasing spectrum in Fig. 4 with dashed curve. As can be seen, the spectrum of the Q-switched operation has a larger bandwidth than that of CW lasing operation. This might be because of the self-phase modulation effect in the laser cavity. It is also observed that the operating

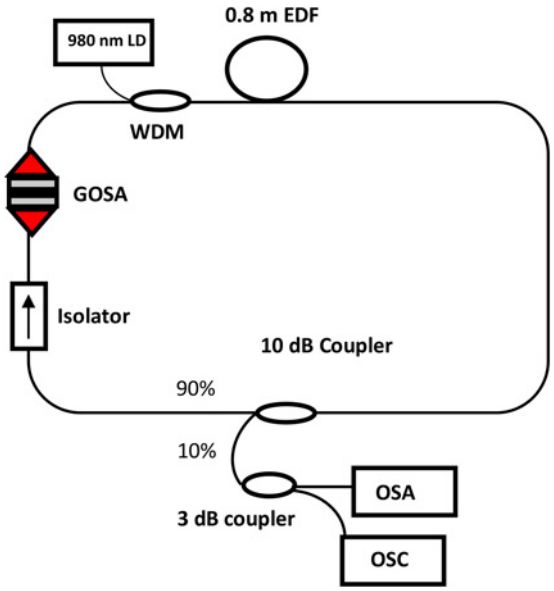

Fig. 3 *Configuration of the proposed Q-switched EDFL*

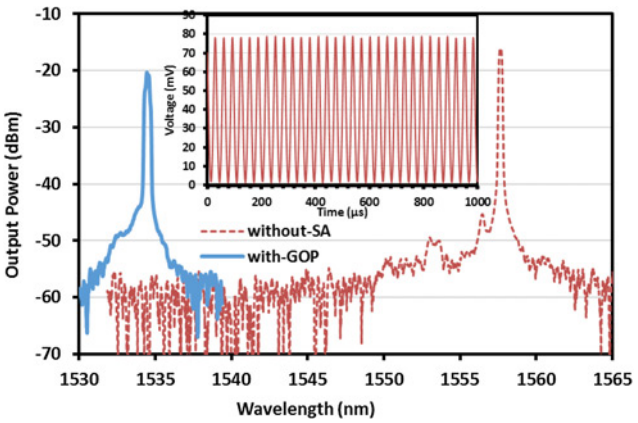

Fig. 4 *Output spectra of the EDFL with and without the GOSA*
Inset shows the typical Q-switching pulse train with the GOSA at pump power of 50.5 mW

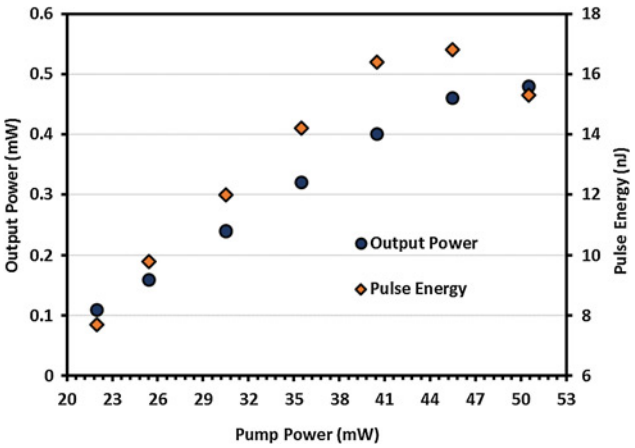

Fig. 6 *Average output power and pulse energy as a function of 980 nm pump power*

wavelength of the laser shifted from 1557.7 to 1534.4 nm with the incorporation of GOSA. This is attributed to the cavity loss, which increases with the incorporation of SA. Therefore the laser operates at a shorter wavelength to acquire more gain to compensate for the loss. Correspondingly, the typical Q-switched pulse train is presented in the inset of Fig. 4 when the pump power is fixed at 50.5 mW. The repetition rate is 31.5 kHz. The pulse duration, which was measured directly from an oscillograph, is about 13.8 μs. There is no distinct amplitude modulation in each Q-switched envelop spectrum in the inset. This indicates that the self-mode-locking effect on the Q-switching is weak for the proposed laser.

We then measured the tuning range of the Q-switched output pulse as a function of pump power. As shown in Figs. 5 and 6, the output pulse width and repetition rate changed when the pump power increased. Such as a typical Q-switched fibre lasers, the pulse repetition rate increases from 14.3 to 31.5 kHz with increasing pump power from 22 to 50.5 mW. On the other hand, the pulse width decreases from 32.8 to 13.8 μs as the pump power is increased within the same range. This effect is because of gain compression in the Q-switched fibre laser. Further reduction in pulse width is expected by shortening the cavity length using a higher dopant fibre. Inset of Fig. 5 shows the RF spectrum of the Q-switched laser at pump power of 50.5 mW. It shows that the laser operates at a repetition rate of 31.4 kHz with an SNR of about 12 dB. This indicates the stability of the pulse train generated by the proposed Q-switched EDFL. It is worthy to note that the Q-switching pulse disappears as the pump power is further increased above 50.5 mW.

Fig. 8 shows the average output power and pulse energy of the Q-switched EDFL as functions of pump power. As shown in this figure, the average output power increases from 0.11 to 0.48 mW, whereas the pulse energy fluctuates within 7.7 to 16.8 nJ as the pump power increases from 22 to 50.5 mW. The maximum pulse

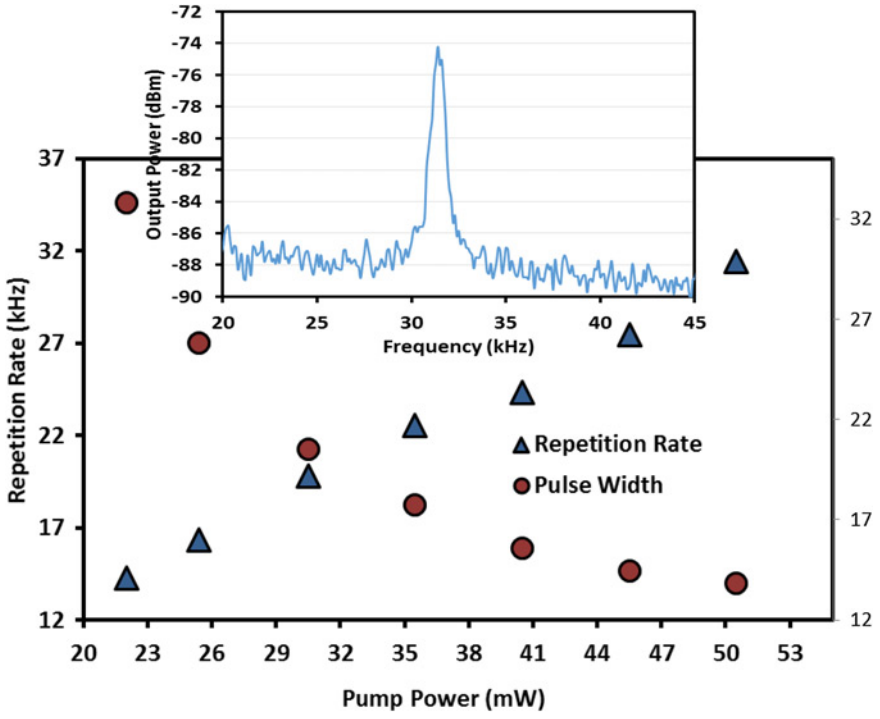

Fig. 5 *Repetition rate and pulse width as a function of 980 nm pump power*
Inset shows the RF spectrum of the Q-switched laser at pump power of 50.5 mW

doi: 10.1049/joe.2014.0321

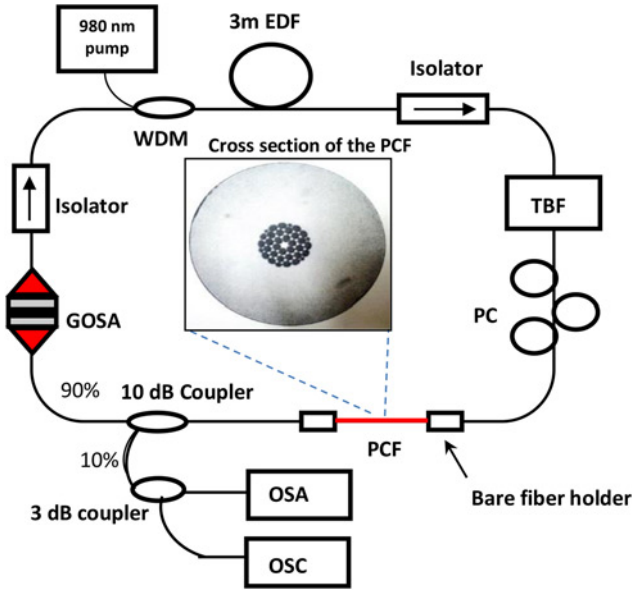

Fig. 7 *Experimental setup of the dual-wavelength Q-switched fibre laser*
Inset shows the cross-section of the PCF

energy of 16.8 nJ is obtained at the pump power of 45.5 mW. We believe that the pulse energy could be improved by reducing the insertion loss of the GOSA and optimising the laser cavity.

4 Dual-wavelength Q-switched EDFL

Many works on all-fibre dual-wavelength fibre lasers (DWFLs) have also been reported in recent years because of interests in their potentials in applications such as optical instrument testing, optical signal processing, fibre sensing systems and microwave photonics. For instance, a dual-wavelength Q-switched fibre lasers were reported by Luo *et al.* [23] in 2010. In this section, a dual-wavelength Q-switched EDFL with a very narrow wavelength spacing of 33 pm is demonstrated by using a GO paper as SA. A tunable bandpass filter (TBF) and a short length of photonics crystal fibre (PCF) are utilised in the cavity to produce the dual-wavelength fibre laser via four-wave-mixing effect.

Fig. 7 shows the experiment setup of a dual-wavelength Q-switched EDFL, which uses a 3 m long EDF as gain medium. By pumping the EDF with a 980 nm laser diode through a WDM, an ASE is generated at C-band, which oscillates in the ring cavity to generate laser. Two isolators are used in the ring cavity to ensure unidirectional light propagation and the stability of the generated laser. A PCF is used to generate a stable and narrow spacing dual-wavelength laser by polarisation dependence loss and fringe spacing effects, where its terminals are mechanically coupled with SMF-28 fibre via the bare fibre holders. In the inset of Fig. 3, a microscopic picture of the PCF's cross-section is shown, having holes with diameter of 5.06 µm and the distance between the centres of each hole is 5.52 µm. It has a core diameter of 4.37 µm and a fibre diameter of 124 µm. To generate dual-wavelength laser, the polarisation controller (PC) is adjusted accordingly to switch the laser polarisation states to a proper state. In addition, a TBF with a bandpass bandwidth of 0.8 nm and tuning resolution of 0.05 nm is employed into the laser cavity to filter the unwanted laser emissions, and bandpass the required dual-wavelength laser. By carefully fine tuning the TBF and PC, a narrow spacing dual-wavelength laser is obtained. A GOSA assembly is then placed inside the laser cavity as a component to generate the Q-switched dual-wavelength laser. A 10 dB coupler is used to tap out 10% of the laser light from the ring cavity.

At first, the generation of the DWFL was obtained by pumping a 66 mW of 980 nm laser from the laser diode into the ring cavity without the GOSA. The optical spectrum of the narrow spacing DWFL was monitored using a high-resolution OSA (APEX AP2051A – with highest resolution of 0.16 pm at a span of 0.164 nm). The PC was fine tuned until dual-wavelength laser was generated and measured from the OSA as shown in Fig. 8*a*, where the spacing between the two wavelengths of 28 pm is obtained with SNR of 53.7 and 3 dB linewidth of about 0.6 pm. After the generation of DWFL with stable output observed, the GOSA was inserted into the ring laser cavity to trigger the Q-switching effect. Fig. 8*b* shows the optical spectrum scan after the GOSA was placed in the cavity. Series of spikes are observed because of the large fluctuation of the optical power at high frequency, while the OSA scanning through each of the wavelength. The Q-switched DWFL obtained has an approximate wavelength spacing of 33 pm and an SNR of 49.6 dB, which differs slightly when operating in CW regime because of the change in the laser polarisation state when the GOSA assembly is inserted.

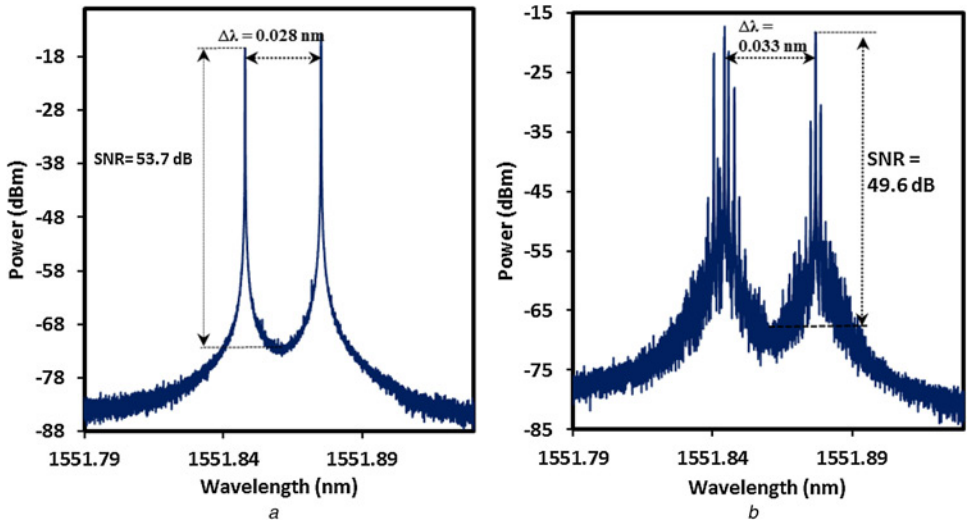

Fig. 8 *Dual-wavelength laser spectra captured using high-resolution OSA*
a CW
b Q-switching with GOSA assembly is employed in the laser cavity

doi: 10.1049/joe.2014.0321

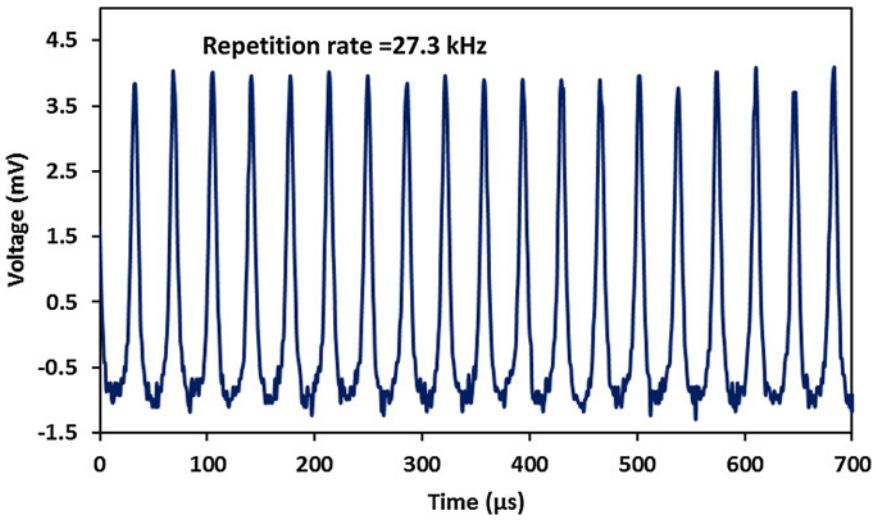

Fig. 9 *Pulse train of the dual-wavelength Q-switched EDFL pumped at 66 mW*

Fig. 9 shows the typical pulse train of the Q-switched DWFL at the pump power of 66 mW. It shows a series of stable pulse train with pulse repetition rate of 27.7 kHz and pulse width of about 7.4 µs at full width half maximum (FWHM). The stability of the Q-switched pulses is then analysed by measuring the power output fluctuation with radio frequency spectrum analyser (RFSA). Fig. 10 shows the first harmonic RF spectrum of the Q-switched DWFL at 20 kHz span, with resolution and video bandwidth of 300 Hz and 1 MHz, respectively. The signal has a peak-to-noise ratio of about 37 dB which confirms pulse stability.

The proposed dual-wavelength Q-switched EDFL offers slight tuning in the repetition rate and pulse width to fulfil different applications which need different pulse specifications. The tuning can be performed by changing the 980 nm pump power. Fig. 11 shows repetition rate and pulse width curves at different pump powers. The threshold to trigger the Q-switching is level at about 54 mW. The repetition rate increases linearly from the threshold to a maximum repetition rate of 31 kHz at the pump power of 69 mW. In contrast, the pulse width decreases with exponent manner from 13.2 µs, reaching to a saturation value of about 7.04 µs at 69 mW pump power. However, further increase in pump power leads to pulse instability and broadening. Since the dual-wavelength laser has a very narrow spacing and broad laser spectrum, the two wavelengths will eventually bound to merge together as the pump power is increased. This contributes to unstable dual-wavelength laser generation which limits the further increase of the pump power for Q-switching operation. Fig. 12 shows the average output power and the calculated pulse energy curves at different pump powers. Both output power and pulse energy increase linearly as the pump power is increased. Under the pump power of 69 mW, the average output power of 0.086 mW and pulse energy of 2.8 nJ are obtained.

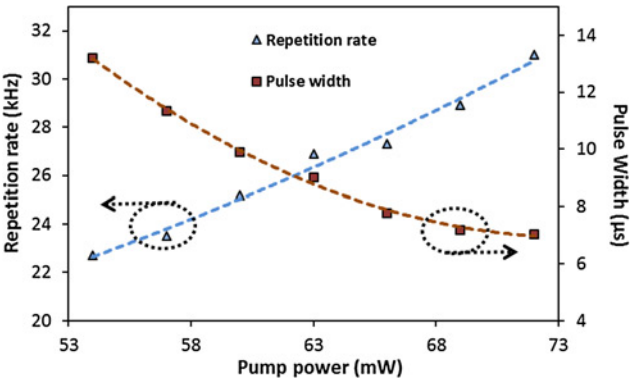

Fig. 11 *Repetition rate and pulse width curves at different pump powers*

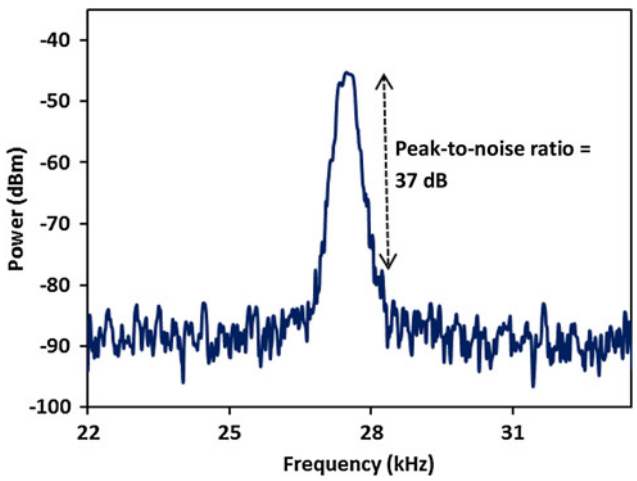

Fig. 10 *First harmonic RF spectrum of the Q-switched DWFL*

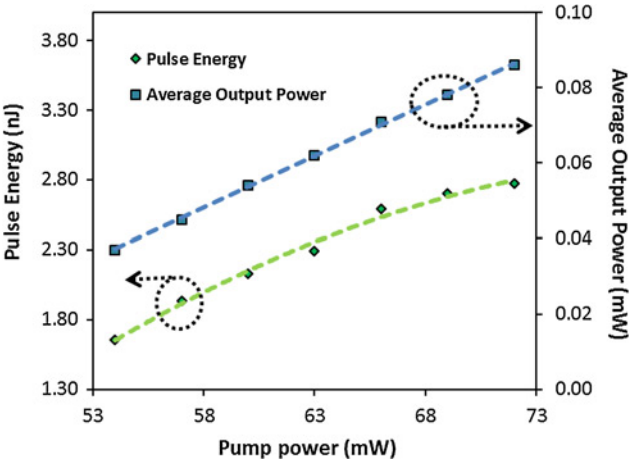

Fig. 12 *Pulse energy and average output power curves at different pump powers*

doi: 10.1049/joe.2014.0321

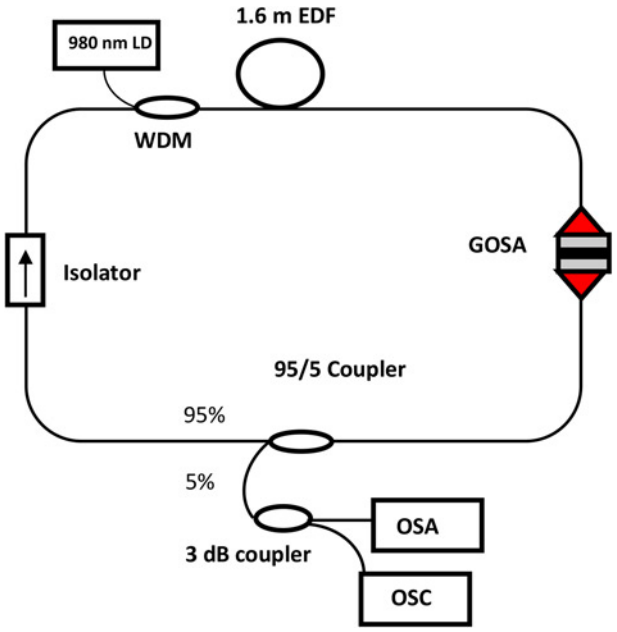

Fig. 13 *Configuration of the proposed mode-locked EDFL*

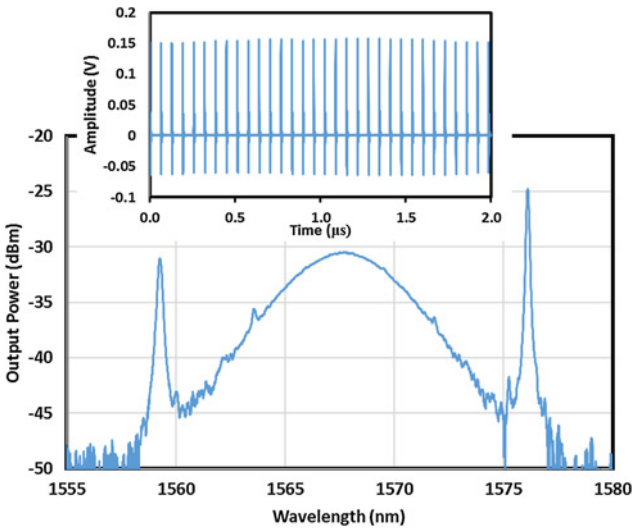

Fig. 14 *Output spectrum of the mode-locked EDFL*
Inset shows the typical pulse train at pump power of 18 mW

5 Mode-locked EDFL with GO paper as an SA

In the previous two sections, Q-switched EDFLs have been demonstrated using the GO paper-based SA. Numerous works have also been reported on graphene-based mode-locked fibre lasers in literatures [10, 16, 29, 30]. Recently, Xu *et al.* [16] has demonstrated a mode-locked femtosecond EDFLs using GOSA. The SA was prepared by immersing a broadband mirror into a GO hydrosol. After 48 h, a thin graphene membrane was formed on top of the broadband reflective mirror. In another work, Sobon *et al.* [18] compares the performances of GO and rGO as SA. The SAs were placed on fused silica substrate and inserted between two collimating gradient index lenses to achieve mode-locked fibre lasers. In this section, we demonstrate a femtosecond mode-locked EDFL using the GO paper as a mode-locker. The paper is sandwiched between two fibre ferrules to initiate mode-locking in the proposed new configuration, which produces soliton pulse train with 15.62 MHz repetition rate and 680 fs pulse width. We observed that the fibre laser has low pulsing threshold as well as low damage threshold. Therefore pulse energy and peak power are 0.0085 nJ and 11.85 W, respectively. The easy fabrication of GO paper will promote its potential in ultrafast photonics applications.

The schematic of the proposed mode-locked EDFL is shown in Fig. 13. It was constructed using a simple ring cavity, in which a 1.6 m long EDF was used instead of 0.8 m or 3 m EDF for Q-switching application. The EDF was forward pumped by a 1480 nm laser diode via a 1480/1550 nm WDM. The polarisation independent isolator was used to ensure unidirectional light propagation in the cavity and thus facilitate self-starting laser. The total length of the laser cavity was measured to be ~12.6 m, comprising 1.6 m EDF and 11 m SMF-28 fibre. The group velocity dispersion (GVD) for the EDF and SMF-28 were −21.64 and 17 ps/nm/km, respectively, at 1550 nm. Therefore the resultant total GVD for this mode-locked fibre laser was estimated to be 0.1513 ps/nm/km. This indicated that the proposed mode-locked fibre laser operated in the anomalous dispersion regime and thus it could be classified as a soliton fibre laser. The laser output was obtained via a 95/5 output coupler located between the isolator and SA, which channelled out about 5% of the oscillating light from the ring cavity. All components used in our setup were polarisation independent, that is, they support any light polarisation. No PC was included in the laser cavity as we had observed earlier that a PC did not improve our pulse stability. There was no significant pulse jitter observed through the oscilloscope during the experiment.

The mode-locked fibre laser had a low self-starting threshold; approximately at 8.7 mW. Fig. 14 shows the spectral profile where the presence of soliton is confirmed. The solitons' central wavelength, λc, is situated at 1567.9 nm and the 3 dB bandwidth is ~7.44 nm with strong Kelly sidebands at 1559.3 and 1576.1 nm. The spectrum is free from CW parasitic lasing. The presence of Kelly sidebands confirms that this mode-lock fibre laser is operating in anomalous dispersion regime. Inset of Fig. 14 shows the typical pulse train of the passive mode-locked fibre laser obtained at pump power of 18 mW. It has a cavity round trip time of 64.1 ns, corresponding to a pulse repetition rate 15.6 MHz and a cavity length of 12.6 m.

Fig. 15 shows the second harmonic generation (SHG) autocorrelation trace, with the estimated pulse duration of 870 fs at its FWHM. The sech² fitting which indicates the generation of the soliton pulse is also included in this figure. The autocorrelation trace reveals that the experimental result follows the sech² fitting closely. Inset of Fig. 15 shows the RF spectrum of the soliton mode-locked EDFL at repetition rate of 15.6 MHz. It shows an SNR of about 70 dB, which indicates the stability of the output pulse train. A time-bandwidth product is calculated to be about 0.78

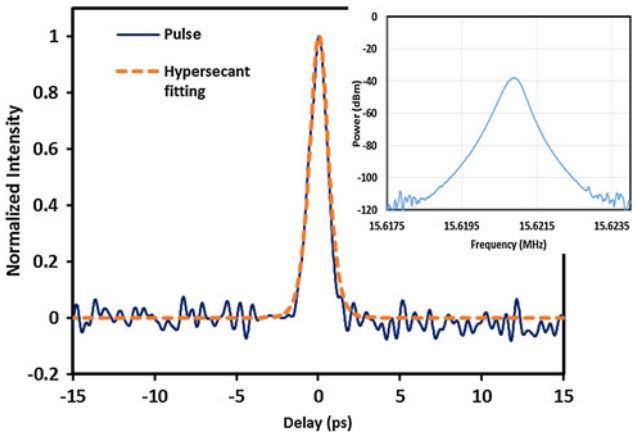

Fig. 15 *SHG autocorrelation trace of the mode-locked laser*
Inset shows the RF spectrum

doi: 10.1049/joe.2014.0321

from the 3 dB bandwidth of the optical spectrum. This shows that the pulse is a chirped pulse. Since the pulsing threshold is low, the output power for this fibre laser is 0.061 mW. Consequently, the resultant pulse energy and peak power are 3.9 pJ and 4.2 W, respectively.

6 Conclusion

In summary, we have successfully demonstrated Q-switched and mode-locked EDFLs by using a commercial non-conductive GO paper as SA. The paper is sandwiched between two fibre ferrules and incorporated into the laser cavity for pulse generation. A Q-switched pulse train was achieved at 1534.4 nm by using a 0.8 m long EDF as gain medium in a ring configuration. The pulse repetition rate changed from 14.3 to 31.5 kHz, whereas the corresponding pulse width decreased from 32.8 to 13.8 μs as the 980 nm pump power was increased from the Q-switching threshold value of 22–50.5 mW. A narrow spacing Q-switched DWFL was also demonstrated using the GOSA. It employed PCF and a TBF in the setup to produce a dual-wavelength laser output with a wavelength spacing of 33 pm and an SNR of about 49.6 dB. The DWFL can operate at a maximum repetition rate of 31 kHz, with its pulse duration of 7.04 μs and pulse energy of 2.8 nJ. We have also successfully demonstrated a soliton mode-locked fibre laser by using a GOSA in a ring cavity comprising of a 1.6 m long EDF, which was pumped by a 1480 nm laser diode. The laser generates a pulse train with a repetition rate of 15.62 MHz, pulse width of 870 fs, pulse energy 3.9 pJ and peak power of 4.2 W. The SA had a relatively low self-starting threshold although susceptible to damage at higher pump power. The SA was only able to withstand pulse operation for a short period of time. Given by the simplicity of preparing a GO paper, these experiments prove that a non-conductive GO paper can be an alternative to existing graphene and GO-based SA.

7 Acknowledgment

This project was funded by the Ministry of Education and University of Malaya under various grant schemes (grant nos. SF014-2014, PG139-2012 B and PG068-2013B).

8 References

[1] Wang Q.Q., Chen T., Zhang B.T., Li M.S., Lu Y.F., Chen K.P.: 'Passively mode-locked all-fiber thulium-doped fiber ring lasers using graphene saturable absorbers', *Appl. Phys. Lett.*, 2013, **102**, p. 131117

[2] Anyi C.L., Haris H., Harun S.W., Ali N.M., Arof H.: 'Nanosecond pulse fiber laser based on nonlinear polarisation rotation effect', *Electron. Lett.*, 2013, **49**, pp. 1240–1241

[3] Wang J., Luo Z., Zhou M., *ET AL.*: 'Evanescent-light deposition of graphene onto tapered fibers for passive Q-switch and mode-locker', *IEEE Photonics J.*, 2012, **4**, (5), pp. 1295–1305

[4] Keller U.: 'Recent developments in compact ultrafast lasers', *Nature*, 2003, **424**, pp. 831–838

[5] Sun Z.P., Hasan T., Torrisi F., *ET AL.*: 'Graphene mode-locked ultrafast laser', *ACS Nano*, 2010, **4**, pp. 803–810

[6] Set S.Y., Yaguchi H., Tanaka Y., Jablonski M.: 'Laser mode locking using a saturable absorber incorporating carbon nanotubes', *J. Lightwave Technol.*, 2004, **22**, (1), pp. 51–56

[7] Martinez A., Sun Z.: 'Nanotube and graphene saturable absorbers for fibre lasers', *Nat. Photonics*, 2013, **7**, pp. 842–845

[8] Bonaccorso F., Sun Z., Hasan T., Ferrari A.: 'Graphene photonics and optoelectronics', *Nat. Photonics*, 2010, **4**, (9), pp. 611–622

[9] Popa D., Sun Z., Hasan T., Torrisi F., Wang F., Ferrari A.C.: 'Graphene Q-switched, tunable fiber laser', *Appl. Phys. Lett.*, 2011, **98**, (7), pp. 073106-1–073106-3

[10] Ugolotti E., Schmidt A., Petrov V., *ET AL.*: 'Graphene mode-locked femtosecond Yb:KLuW laser', *Appl. Phys. Lett.*, 2012, **101**, (16), p. 161112

[11] Dikin D.A., Stankovich S., Zimney E.J., *ET AL.*: 'Preparation and characterization of graphene oxide paper', *Nature*, 2007, **448**, pp. 457–460

[12] Zhu Y., Murali S., Cai W., *ET AL.*: 'Graphene and graphene oxide: synthesis, properties, and applications', *Adv. Mater.*, 2010, **22**, (35), pp. 3906–3924

[13] Zhao X., Liu Z.B., Yan W.B., *ET AL.*: 'Ultrafast carrier dynamics and saturable absorption of solution-processable few-layered graphene oxide', *Appl. Phys. Lett.*, 2011, **98**, (12), p. 121905

[14] Loh K.P., Bao Q.L., Eda G., Chhowalla M.: 'Graphene oxide as a chemically tunable platform for optical applications', *Nat. Chem.*, 2010, **2**, (12), pp. 1015–1024

[15] Xu J., Wu S., Li H., *ET AL.*: 'Dissipative soliton generation from a graphene oxide mode-locked Er-doped fiber laser', *Opt. Express*, 2012, **20**, (21), pp. 23653–23658

[16] Xu J., Liu J., Wu S., Yang Q.–H., Wang P.: 'Graphene oxide mode-locked femtosecond erbium-doped fiber lasers', *Opt. Express*, 2012, **20**, (14), pp. 15474–15480

[17] Liu Z.B., He X.Y., Wang D.N.: 'Passively mode-locked fiber laser based on a hollow-core photonic crystal fiber filled with few-layered graphene oxide solution', *Opt. Lett.*, 2011, **36**, (16), pp. 3024–3026

[18] Sobon G., Sotor J., Jagiello J., *ET AL.*: 'Graphene oxide vs. reduced graphene oxide as saturable absorbers for Er-doped passively mode-locked fiber laser', *Opt. Express*, 2012, **20**, (17), pp. 19463–19473

[19] Wang Y.G., Qu Z.S., Liu J., Tsang Y.H.: 'Graphene oxide absorbers for watt-level high-power passive mode-locked Nd:GdVO4 laser operating at 1 μm', *J. Lightwave Technol.*, 2012, **30**, (20), pp. 3259–3262

[20] Feng C., Liu D., Liu J.: 'Graphene oxide saturable absorber on golden reflective film for Tm:YAP Q-switched mode-locking laser at 2 μm', *J. Mod. Opt.*, 2012, **59**, pp. 1825–1828

[21] Wang Y.G., Chen H.R., Hsieh W.F., Tsang Y.H.: 'Mode-locked Nd:GdVO4 laser with graphene oxide/polyvinyl alcohol composite material absorber as well as an output coupler', *Opt. Commun.*, 2013, **289**, pp. 119–122

[22] He X., Liu Z.-B., Wang D., Yang M., Liao C.R., Zhao X.: 'Passively mode-locked fiber laser based on reduced graphene oxide on microfiber for ultra-wide-band doublet pulse generation', *J. Lightwave Technol.*, 2012, **30**, (7), pp. 984–989

[23] Luo Z., Zhou M., Weng J., *ET AL.*: 'Graphene-based passively Q-switched dual-wavelength erbium-doped fiber laser', *Opt. Lett.*, 2010, **35**, (21), pp. 3709–3711

[24] Dong X., Su C.-Y., Zhang W., *ET AL.*: 'Ultra-large single-layer graphene obtained from solution chemical reduction and its electrical properties', *Phys. Chem. Chem. Phys.*, 2010, **12**, (9), pp. 2164–2169

[25] Huang N.M., Lim H.N., Chia C.H., Yarmo M.A., Muhamad M.R.: 'Simple room-temperature preparation of high-yield large-area graphene oxide', *Int. J. Nanomed.*, 2011, **6**, pp. 3443–3448

[26] Jorio A., Saito R., Dresselhaus G., Dresselhaus M.S., Dresselhaus G.: 'Raman spectroscopy in graphene related systems' (WILEY-VCH Verlag GmbH & Co. KGaA, Germany, 2011)

[27] Ferrari A.C., Robertson J.: 'Interpretation of Raman spectra of disordered and amorphous carbon', *Phys. Rev. B*, 2000, **61**, (20), pp. 14095–14107

[28] Shichao Z., Sumedh P.S., Zhiting L., Haitao L.: 'Photochemical oxidation of CVD-grown single layer graphene', *Nanotechnology*, 2012, **23**, (35), p. 355703

[29] Cao W.J., Wang H.Y., Luo A.P., Luo Z.C., Xu W.C.: 'Graphene-based, 50 nm wide-band tunable passively Q-switched fiber laser', *Laser Phys. Lett.*, 2012, **9**, (1), pp. 54–58

[30] Liu J., Wu S., Yang Q., Song Y., Wang Z., Wang P.: '163 nJ graphene mode-locked Yb-doped fiber laser'. CLEO:2011 – Laser Applications to Photonic Applications, OSA Technical Digest (CD), 2011, paper JWA23